Time-Optimal Trajectory Planning for Delta Robot Based on Quintic Pythagorean-Hodograph Curves

TINGTING SU[1,2], **LONG CHENG**[2,3], **(Senior Member, IEEE), YUNKUAN WANG**[1,2],
XU LIANG[2,3]**, JUN ZHENG**[1]**, AND HAOJIAN ZHANG**[1,2]
[1]Intelligent Manufacturing Technology and System Research Center, Institute of Automation, Chinese Academy of Sciences, Beijing 100190, China
[2]School of Artificial Intelligence, University of Chinese Academy of Sciences, Beijing 100049, China
[3]State Key Laboratory of Management and Control for Complex Systems, Institute of Automation, Chinese Academy of Sciences, Beijing 100190, China

Corresponding author: Long Cheng (long.cheng@ia.ac.cn)

ABSTRACT In this paper, a time-optimal trajectory planning method based on quintic Pythagorean-Hodograph (PH) curves is proposed to realize the smooth and stable high-speed operation of the Delta parallel robot. The trajectory is determined by applying the quintic PH curves to the transition segments in the pick-and-place operation trajectory and the 3-4-5 polynomial motion law to the trajectory. The quintic PH curves are optimized to reduce the cycle time of the pick-and-place operation. In addition, a comparison between different trajectory planning methods has been implemented so as to observe the performance of the obtained results. The MATLAB simulation results reveal that compared with the trajectory planning based on vertical and horizontal motion superposition, the trajectory planning based on quintic PH curves is completed with a shorter motion cycle time and more stable motion performance, with the velocities, accelerations, and jerks in joint space bounded and continuous. Experiments carried out on the prototype also confirm that the trajectory planning based on quintic PH curves has a shorter cycle time, which is of great importance to high-speed operations of Delta parallel robots.

INDEX TERMS Delta parallel robot, pick-and-place operation, trajectory planning, quintic Pythagorean-Hodograph curves, optimization.

I. INTRODUCTION

As one of the most successful parallel mechanisms, the Delta robot [1], [2] is a type of parallel robot [3]–[6] with high velocity, accurate positioning, low cost and high efficiency [7]. It is widely used in production lines of food, medicine and electronic products in order to complete rapid sorting, grabbing, assembly and so on [8]. Due to its outstanding dynamic performance [9], it is commonly used to execute pick-and-place operation in production lines. Pick-and-place is known as one of the key operations in programmable assembly where items are selectively picked up and placed in their respective positions. It can be applied to various areas such as palletizing, warehousing, loading/unloading machine, machine tending, sorting, circuit board testing, inspection and remote maintenance, and robotic surgery, in food, pharmaceutical, biomedical, packaging, electrical, and chemical industries [10]. However, it is often difficult for a robot to automatically plan its pick-and-place motion [11]. Therefore, it is of great significance to research the

pick-and-place operation trajectory for high-speed Delta robot. There has been an intense interest in proposing new approaches to obtaining the optimal trajectories of parallel manipulators [12]–[15], whereas little attention has been paid to optimizing the trajectories for Delta robots. Afroun *et al.* [16] presented an approach to planning optimal trajectories of Delta robots in which the operational coordinates of the moving platform were parameterized and the sequential quadratic programming method was applied to find the optimal solutions. Xie *et al.* [17] proposed a trajectory planning approach for Delta robots in pick-and-place operation in which the transitions between the vertical and horizontal segments of the trajectory were smoothed with Lamé curves. The approach reduced the residual vibration of the mechanism, but the calculation was complex and the time performance was comparatively poor.

With the advantage of expressing the arc length as a polynomial function of curve parameter, Pythagorean-Hodograph (PH) curves have been widely studied in path

planning [18]. Farouki and Sakkalis [19] proposed the Pythagorean-Hodograph curves in 1990, in order to establish the exact relationship between the curve parameter and the arc length of the curve. PH curves are a special family of free-form parametric curves and a subset of the Bezier representation, which have the advantage that the arc length can be expressed as a polynomial function of curve parameter. Because of its unique advantages, PH curves are widely applied in high-speed CNC machining, the tool path offset design and radius compensation, the analysis of computer geometric tolerance, traffic line design and many other fields [20]–[23]. Zeng *et al.* [24] proposed a new approach based on PH curves and modified harmony search algorithm to solve the two-stage path-planning problem subject to kinematic constraints for multiple car-like robots. A quintic PH curve was used by Farouki and Nittler [25] to meet the incoming/outgoing path segments with G(2) continuity. Jahanpour and Imani [26] adopted real-time PH curve CNC interpolator for high speed corner machining in order to decrease the corner error.

Nevertheless, few studies have applied PH curves to trajectory planning for Delta robot. On this basis, taking Delta parallel robot as the research object, this paper proposed a PH curves based trajectory planning method for the pick-and-place operation. The quintic PH curves are applied to the transition segments in the pick-and-place operation trajectory, and the 3-4-5 polynomial motion law is utilized to plan the trajectory. The transition segments are formed by the quintic PH curves to guarantee that the velocities, accelerations and jerks in joint space are bounded and continuous. In order to make the robot have a short motion period and a good motion performance, the PH curves are optimized to reduce the cycle time. The trajectory planning based on vertical and horizontal motion superposition is also presented as a comparison method to make comparisons.

The remainder of this paper is organized as follows: Section II presents the trajectory planning based on quintic PH curves, including quantic PH curves, polynomial acceleration and deceleration motion law, trajectory optimization, trajectory planning and self-optimizing trajectory in constrained space. Section III presents the trajectory planning based on vertical and horizontal motion superposition. Experimental and simulation results and analysis are presented in Section IV. Section V gives the conclusions.

II. TRAJECTORY PLANNING METHOD BASED ON QUINTIC PH CURVES

The Delta parallel robot is shown in Figure 1. The schematic of the pick-and-place operation system is illustrated in Figure 2, in which the Delta robot is used to pick the workpiece up from the conveyer belt and place it in the target position. The pick-and-place operation path is shown in Figure 3. The path [9] is represented as *ABCDEFG*. In the horizontal direction, $|AG| = w$, $|HC| = |EI| = r$, in the vertical direction, $|AH| = |GI| = h$, $|AB| = |GF| = j$,
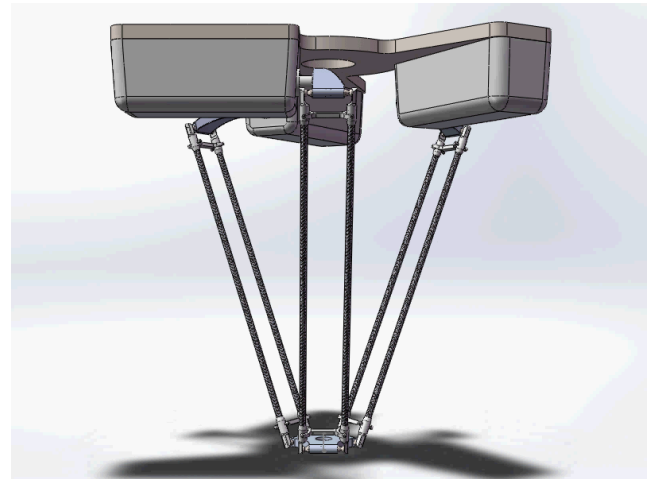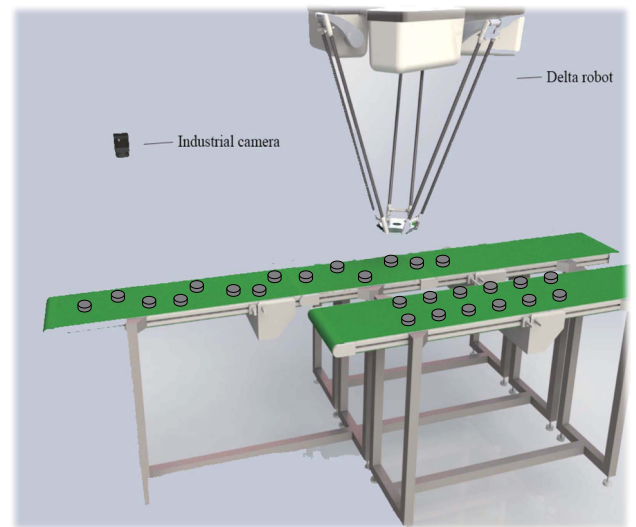

FIGURE 1. Delta parallel robot.

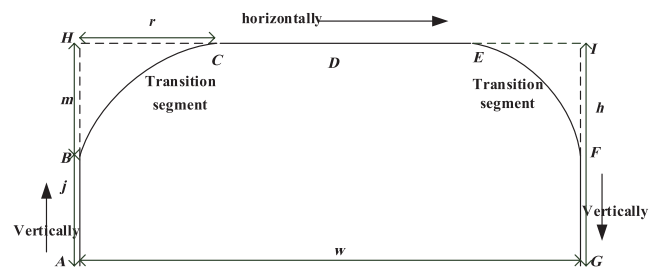**FIGURE 2.** Schematic of the pick-and-place operation system.

FIGURE 3. Pick-and-place operation path.

$|BH| = |FI| = m$. The transition segments *BC* and *EF* of the path are formed by quintic PH curves.

A. QUINTIC PH CURVES
The Bezier representation of PH curves can be defined as:

$$P(\gamma) = (x(\gamma), y(\gamma)) = \sum_{i=0}^{n} \binom{n}{i} P_i \gamma^i (1-\gamma)^{n-i}, \quad \gamma \in [0, 1],$$
(1)

where $P_i = (x_i, y_i)$ is the control point of the curve, $i = 0 \ldots n$, n is the degree of the curve, γ is the curve parameter. If there exists a polynomial $\sigma(\gamma)$ that satisfies:

$$\|P'(\gamma)\| = \sqrt{x'^2(\gamma) + y'^2(\gamma)} = \sigma(\gamma), \qquad (2)$$

then $P(\gamma) = (x(\gamma), y(\gamma))$ is a PH curve of degree n. $x'(\gamma)$, $y'(\gamma)$ and $\sigma(\gamma)$ form a pythagorean triangle. $x'(\gamma)$ and $y'(\gamma)$ can be defined as the one in [27]:

$$\begin{cases} x'(\gamma) = w(\gamma)(u^2(\gamma) - v^2(\gamma)) \\ y'(\gamma) = 2w(\gamma)u(\gamma)v(\gamma). \end{cases} \qquad (3)$$

Generally assume that $w(\gamma) = 1$ can guarantee that the curve has no cusp and the PH curve is odd. Therefore:

$$\sigma(\gamma) = u^2(\gamma) + v^2(\gamma). \qquad (4)$$

The key to construct the PH curve is to determine $u(\gamma)$ and $v(\gamma)$. For the quintic PH curves, $u(\gamma)$ and $v(\gamma)$ are expressed as:

$$\begin{cases} u(\gamma) = u_0(1-\gamma)^2 + 2u_1(1-\gamma)\gamma + u_2\gamma^2 \\ v(\gamma) = v_0(1-\gamma)^2 + 2v_1(1-\gamma)\gamma + v_2\gamma^2. \end{cases} \qquad (5)$$

In this paper, the transition segments of the pick-and-place operation path are formed by quintic PH curves. The quintic PH curves are:

$$P(\gamma) = (x(\gamma), y(\gamma)) = \sum_{i=0}^{5} \binom{5}{i} P_i \gamma^i (1-\gamma)^{5-i}, \gamma \in [0, 1]. \qquad (6)$$

The control points of the quintic PH curve are:

$$\begin{cases} P_1 = P_0 + \dfrac{1}{5}(2u_0v_0, u_0^2 - v_0^2) \\[2mm] P_2 = P_1 + \dfrac{1}{5}(u_0v_1 + u_1v_0, u_0u_1 - v_0v_1) \\[2mm] P_3 = P_2 + \dfrac{2}{15}(2u_1v_1, u_1^2 - v_1^2) \\[2mm] \qquad + \dfrac{1}{15}(u_0v_2 + u_2v_0, u_0u_2 - v_0v_2) \\[2mm] P_4 = P_3 + \dfrac{1}{5}(u_1v_2 + u_2v_1, u_1u_2 - v_1v_2) \\[2mm] P_5 = P_4 + \dfrac{1}{5}(2u_2v_2, u_2^2 - v_2^2). \end{cases} \qquad (7)$$

Figure 4 shows the transition segment BC based on PH curve and the coordinate system XOY. To solve the quintic PH curve, u_0, u_1, u_2, v_0, v_1 and v_2 should be calculated. To simplify the calculation, P_0P_1 is assumed to be on the Y
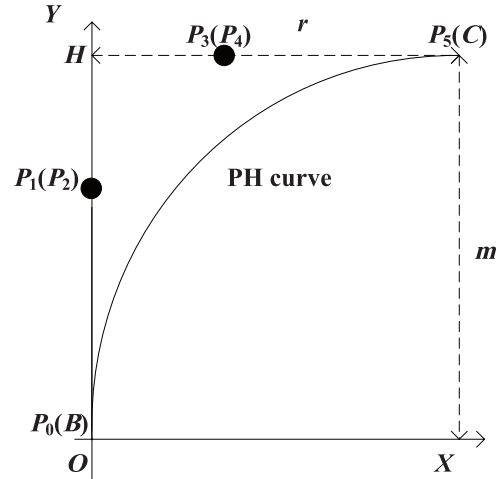
FIGURE 4. Quintic PH curve and its coordinate system *XOY*.

axis. Therefore $v_0 = 0$ and the simplified equation is:

$$\begin{cases} P_1 = P_0 + \dfrac{1}{5}(0, u_0^2) \\[2mm] P_2 = P_1 + \dfrac{1}{5}(u_0v_1, u_0u_1) \\[2mm] P_3 = P_2 + \dfrac{1}{15}(4u_1v_1 + u_0v_2, 2u_1^2 - 2v_1^2 + u_0u_2) \\[2mm] P_4 = P_3 + \dfrac{1}{5}(u_1v_2 + u_2v_1, u_1u_2 - v_1v_2) \\[2mm] P_5 = P_4 + \dfrac{1}{5}(2u_2v_2, u_2^2 - v_2^2). \end{cases} \qquad (8)$$

According to the properties of the PH curves, the curvature k can be calculated as:

$$k(\gamma) = \frac{P'(\gamma) \times P''(\gamma)}{\|P'(\gamma)\|^3} = \frac{4u_0v_2(\gamma - \gamma^2)}{(u^2(\gamma) + v^2(\gamma))^2} \qquad (9)$$

Since $k(0) = 0$ and $k(1) = 0$, it can be calculated that $v_1 = 0$ and $u_1 = 0$. So the further simplified equation is:

$$\begin{cases} P_1 = P_0 + \dfrac{1}{5}(0, u_0^2) \\[2mm] P_2 = P_1 \\[2mm] P_3 = P_2 + \dfrac{1}{15}(u_0v_2, u_0u_2) \\[2mm] P_4 = P_3 \\[2mm] P_5 = P_4 + \dfrac{1}{5}(2u_2v_2, u_2^2 - v_2^2). \end{cases} \qquad (10)$$

The quintic PH curve passes through the first control point and the sixth control point. It can be expressed as:

$$\begin{cases} P(0) = P_0 \\ P(1) = P_5. \end{cases} \qquad (11)$$

By combining equation (10) with equation (11), the control points are obtained as:

$$\begin{cases} P_0 = (0,0) \\ P_1 = (0, \dfrac{1}{5}u_0^2) \\ P_2 = (0, \dfrac{1}{5}u_0^2) \\ P_3 = (\dfrac{1}{15}u_0v_2, \dfrac{1}{5}u_0^2 + \dfrac{1}{15}u_0u_2) \\ P_4 = (\dfrac{1}{15}u_0v_2, \dfrac{1}{5}u_0^2 + \dfrac{1}{15}u_0u_2) \\ P_5 = (\dfrac{1}{15}u_0v_2 + \dfrac{2}{5}u_2v_2, \dfrac{1}{5}u_0^2 + \dfrac{1}{15}u_0u_2 + \dfrac{1}{5}u_2^2 - \dfrac{1}{5}v_2^2). \end{cases} \tag{12}$$

The geometric relationship shown in Figure 4 can be expressed as:

$$\begin{cases} \dfrac{1}{5}u_0^2 + \dfrac{1}{15}u_0u_2 + \dfrac{1}{5}u_2^2 - \dfrac{1}{5}v_2^2 = m \\ \dfrac{1}{15}u_0v_2 + \dfrac{2}{5}u_2v_2 = r \\ \dfrac{1}{5}u_2^2 - \dfrac{1}{5}v_2^2 = 0. \end{cases} \tag{13}$$

So the solution is as follows:

$$\begin{cases} u_0 = \sqrt{\dfrac{5(35m + r - \sqrt{m^2 + r^2 + 70mr})}{34}} \\ u_2 = \sqrt{\dfrac{5(m + 35r - \sqrt{m^2 + r^2 + 70mr})}{68}} \\ v_2 = \sqrt{\dfrac{5(m + 35r - \sqrt{m^2 + r^2 + 70mr})}{68}}. \end{cases} \tag{14}$$

The X and Y coordinates of the quintic PH curve calculated from equation (6) are:

$$\begin{cases} x(\gamma) = \dfrac{2}{3}u_0v_2\gamma^3(1-\gamma)^2 + \dfrac{1}{3}u_0v_2\gamma^4(1-\gamma) \\ \quad + (\dfrac{1}{15}u_0v_2 + \dfrac{2}{5}u_2v_2)\gamma^5 \\ \quad = \dfrac{2}{5}(u_0v_2 + u_2v_2)\gamma^5 - u_0v_2\gamma^4 + \dfrac{2}{3}u_0v_2\gamma^3 \\ y(\gamma) = u_0^2\gamma(1-\gamma)^4 + 2u_0^2\gamma^2(1-\gamma)^3 \\ \quad + (2u_0^2 + \dfrac{2}{3}u_0u_2)\gamma^3(1-\gamma)^2 \\ \quad + (u_0^2 + \dfrac{1}{3}u_0u_2)\gamma^4(1-\gamma) + (\dfrac{1}{5}u_0^2 + \dfrac{1}{15}u_0u_2)\gamma^5. \end{cases} \tag{15}$$

$||P'(\gamma)||$ can be calculated by equation (2) as:

$$\begin{aligned} ||P'(\gamma)|| &= \sqrt{x'^2(\gamma) + y'^2(\gamma)} = \sigma(\gamma) \\ &= u^2(\gamma) + v^2(\gamma) \\ &= (u_0^2 + 2u_0u_2 + u_2^2 + v_2^2)\gamma^4 - (4u_0^2 + 4u_0u_2) \cdot \\ &\quad \gamma^3 + (6u_0^2 + 2u_0u_2)\gamma^2 - 4u_0^2\gamma + u_0^2. \end{aligned} \tag{16}$$

Then the arc length of the quintic PH curve can be calculated as:

$$\begin{aligned} l(\varepsilon) &= \int_0^\varepsilon \sqrt{x'^2(\gamma) + y'^2(\gamma)}\,d\gamma \\ &= (u_0^2 + 2u_0u_2 + u_2^2 + v_2^2)\dfrac{\varepsilon^5}{5} - (4u_0^2 + 4u_0u_2)\dfrac{\varepsilon^4}{4} \\ &\quad + (6u_0^2 + 2u_0u_2)\dfrac{\varepsilon^3}{3} - 4u_0^2\dfrac{\varepsilon^2}{2} + u_0^2\varepsilon. \end{aligned} \tag{17}$$

Therefore:

$$\begin{aligned} l_{\widehat{P_0P_5}} = l_{\widehat{BC}} &= \int_0^1 \sqrt{x'^2(\gamma) + y'^2(\gamma)}\,d\gamma \\ &= \dfrac{1}{5}u_0^2 + \dfrac{1}{15}u_0u_2 + \dfrac{1}{5}u_2^2 + \dfrac{1}{5}v_2^2. \end{aligned} \tag{18}$$

B. 3-4-5 POLYNOMIAL ACCELERATION AND DECELERATION MOTION LAW

In this paper, the robot uses the polynomial acceleration and deceleration motion law in the pick-and-place operation path planning. The following two acceleration and deceleration motion laws, the 3-4-5 polynomial one [28]–[30] and the 3-4-5-6 asymmetric one [31] can both generate trajectories that are continuously differentiable in third order. In comparison, the 3-4-5 polynomial motion law is selected due to its simplicity to implement and its smaller maximum angular acceleration.

Combined with the boundary conditions, the 3-4-5 polynomial motion law can be computed as following:

$$p(\Phi) = l_{all}(6\Phi^5 - 15\Phi^4 + 10\Phi^3), \tag{19}$$

where $\Phi = t/T$ and $\Phi \in [0, 1]$, l_{all} is the total length of the path as shown in Figure 3, t is the time, T is the motion cycle time, which represents the time for a single pick-and-place operation.

The length of the quintic PH curve is $l_{\widehat{BC}} = \frac{1}{5}u_0^2 + \frac{1}{15}u_0u_2 + \frac{2}{5}u_2^2$. The path length l_{all} of the pick-and-place operation trajectory is:

$$l_{all} = 2j + 2l_{\widehat{BC}} + w - 2r. \tag{20}$$

In the pick and place operation, the trajectory can be calculated as:

$$s(t) = p(\Phi). \tag{21}$$

C. TRAJECTORY OPTIMIZATION

The motion cycle time T can be calculated by the motion law (21) as:

$$\begin{aligned} T &= \sqrt{\dfrac{10l_{all}}{\sqrt{3}a_{max}}} \\ &= \sqrt{\dfrac{10(2j + 2l_{\widehat{BC}} + w - 2r)}{\sqrt{3}a_{max}}} \\ &= \sqrt{\dfrac{10(2h + w + 4/34 \cdot \psi)}{\sqrt{3}a_{max}}}, \end{aligned} \tag{22}$$

where $\alpha = \sqrt{m^2 + r^2 + 70mr}$, $\beta = m^2 + r^2 + 36mr$, $\zeta = m + r$, $\psi = \zeta - \alpha + \sqrt{0.5(\beta - \alpha \cdot \zeta)}$, $0 \le m \le h$, $0 \le r \le w/2$, $a_{\max}$ is the maximum acceleration.

In the pick-and-place operation, the constraints are:

$$\begin{cases} q_i^{\min} \le q_i \le q_i^{\max}, i = 1, 2, 3 \\ \dot{q}_i^{\min} \le \dot{q}_i \le \dot{q}_i^{\max}, i = 1, 2, 3 \\ \ddot{q}_i^{\min} \le \ddot{q}_i \le \ddot{q}_i^{\max}, i = 1, 2, 3 \\ |\tau_i| \le \tau_{\max}, i = 1, 2, 3 \\ other\ constraints, \end{cases} \quad (23)$$

where q_i is the ith joint angle, τ_i is the ith motor torque. The torque constraints can be obtained by using dynamic model [1], [32]. Joint position and joint velocity constraints can be satisfied readily, which can be obtained by using kinematic model [1], [31]. Different m and r will make different PH curves. Considering the demand of high-speed operation, T needs to be minimized, which means that the trajectory should achieve the required motions in a time-efficient manner subject to the kinematic and dymamic constraints imposed by the Delta robot mechanism [33].

D. TRAJECTORY PLANNING

It could be computed from "Trajectory optimization" section with the interior point method:

1) The trajectory contains two phases that are both quintic PH curves.
2) $|AB| = |GF| = 0$, $|CE| = 0$.

Figure 5 illustrates the two-phase optimized trajectory:

1) When the end effector of the Delta robot moves from point A to point D, which means $0 \le s(t) \le l_{\overset{\frown}{BC}}$, the robot moves along the quintic PH curve.
2) When the end effector moves from point D to point G, which means $l_{\overset{\frown}{BC}} < s(t) \le 2l_{\overset{\frown}{BC}}$, the robot also moves along the quintic PH curve. At this time, the calculation method of the trajectory coordinates is similar to the calculation method of time (1).
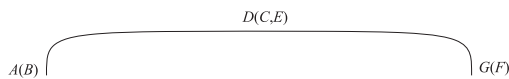
FIGURE 5. Optimized pick-and-place operation trajectory.

The transformation matrix from the *XOY* coordinate system in Figure 4 to the robot base coordinate system $O_R X_R Y_R Z_R$ is required. It can be expressed as:

$$\begin{pmatrix} x_R \\ y_R \\ z_R \\ 1 \end{pmatrix} = \begin{pmatrix} r_{11} & r_{12} & r_{13} & t_1 \\ r_{21} & r_{22} & r_{23} & t_2 \\ r_{31} & r_{32} & r_{33} & t_3 \\ 0 & 0 & 0 & 1 \end{pmatrix} \begin{pmatrix} x \\ y \\ 0 \\ 1 \end{pmatrix} = T_o \begin{pmatrix} x \\ y \\ 0 \\ 1 \end{pmatrix}, \quad (24)$$

where T_o is the transformation matrix from the *XOY* coordinate system to the robot base coordinate system $O_R X_R Y_R Z_R$. By substituting the coordinates of point B, point C, point

P_1 and point P_3 under the *XOY* coordinate system and $O_R X_R Y_R Z_R$ coordinate system into equation (24), T_o can be calculated.

The detailed steps for calculating the coordinates of the robot base coordinate system in the above time (1) are as follows:

1) Calculate $s(t)$ according to equation (21);
2) Obtain the curve parameter γ by combining $s(t)$ with equation (17);
3) Taking γ into equation (15), the coordinates in *XOY* coordinate system could be calculated;
4) Taking the above coordinates into equation (24), the coordinates in the robot base coordinate system will be obtained. The robot base coordinate system is defined in literature [34].

E. TRAJECTORY SELF-OPTIMIZATION IN CONSTRAINED SPACE

The workspace of the DELTA robot is defined as a region in the three-dimensional cartesian space that can be reached by the robot's end-effector [34]. When the trajectory is beyond the constrained workspace, the trajectory should be replanned. Therefore, a trajectory self-optimization method is proposed, which is suitable for constraint workspace and is based on the artificial potential field [35], [36].

1) When the picking or placing point is beyond the constrained space, the artificial potential field could be written as $U_{total}(p) = U_d(p) + U_c(p)$, where p means the current position, $U_d(p)$ is designed to track the desired position, $U_c(p)$ is designed to avoid moving beyond the constrained space. $U_d(p)$ could be defined as $U_d(p) = \frac{1}{2}k_d\|p - p_i\|^2$, where k_d is a positive constant, p_i is the desired picking or placing point. $U_c(p)$ could be defined as $U_c(p) = k_c/d^2$, where k_c is a positive constant, d is the distance from the point p to the boundary of the workspace. p_i could be viewed as the attractive point potential source, and the boundary of the workspace could be viewed as the rejective point potential source. The force F_{total} is given by the negative gradient of the potential:

$$F_{total} = -\nabla U_d - \nabla U_c. \quad (25)$$

After the new picking or placing point is obtained, the method mentioned in "Trajectory planning" section will be used to plan the trajectory.

2) When the transition curve in the desired trajectory is beyond the constrained space, h will be redefined.
3) Repeating step (1) and step (2) until the trajectory is not beyond the constrained space.

However, if the workpiece cannot be picked with the self-optimized trajectory, the task will be terminated.

III. TRAJECTORY PLANNING BASED ON VERTICAL AND HORIZONTAL MOTION SUPERPOSITION

The trajectory planning based on vertical and horizontal motion superposition is commonly used to generate the

curve transition through the motion superposition in different directions.

In this trajectory planning method, the robot adopts the 3-4-5 polynomial motion law in the horizontal direction and vertical direction. The trajectory is shown in Figure 3. Assume T_1 is the motion time from A to C, T_2 is the motion time from B to F, T_3 is the motion time from E to G. So $T_1 = T_3$. There are two cases:

1) $h \leq w$: When $t = 0$, the end effector of the Delta robot starts to move upward in the vertical direction; when $t = T_1/2$, the end effector starts to move in the horizontal direction; when $t = T_2$, the end effector starts to move downward in the vertical direction. Therefore the cycle time T is:

$$T = T_2 + T_3 = \sqrt{\frac{10w}{\sqrt{3}a_{\max}}} + \sqrt{\frac{10h}{\sqrt{3}a_{\max}}}. \quad (26)$$

2) $h > w$: when $t = 0$, the end effector starts to move upward in the vertical direction; when $t = T_1 - T_2/2$, the end effector starts to move in the horizontal direction; when $t = T_1$, the end effector starts to move downward in the vertical direction. Therefore the cycle time T is :

$$T = T_1 + T_3 = 2\sqrt{\frac{10h}{\sqrt{3}a_{\max}}}. \quad (27)$$

IV. EXPERIMENTAL AND SIMULATION RESULTS
A. SIMULATION AND ANALYSIS
The proposed method was tested with MATLAB to perform the numerical simulations. According to the Adeptcycle [37], when the starting point coordinates were (−152.5mm, 0, −800mm), the target point coordinates were (152.5mm, 0, −800mm) and h was 25mm, the trajectory planning based on quintic PH curves and the trajectory planning based on motion superposition were respectively simulated.

The paths in the robot base coordinate system of the above two methods are shown in Figure 6. Figure 7 shows the time responses of the velocities, accelerations and jerks of the end effector during the pick-and-place operation based on quintic PH curves. Figure 8 shows the time responses of the velocities, accelerations and jerks of the end effector in Cartesian space during the pick-and-place operation based on motion superposition.

In addition, the kinematic model was established and its simulation was carried out. During the pick-and-place operation based on quintic PH curves, the angular positions, angular velocities, angular accelerations and angular jerks in joint space are shown in Figure 9. Figures 10 illustrates the angular positions, angular velocities, angular accelerations and angular jerks with the pick-and-place operation based on motion superposition.

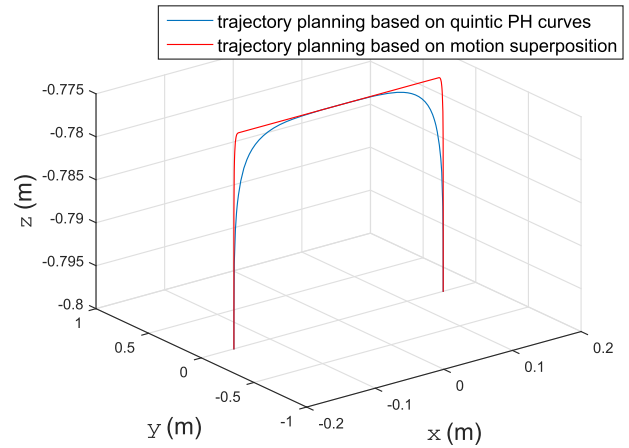The trajectory planning based on quintic PH curves achieves a smooth trajectory as shown in Figure 6. It can

FIGURE 6. Paths planned by the proposed two methods.

be found that the jerks in the trajectory planning based on motion superposition are discontinuous from Figure 8, while the jerks in the trajectory planning based on quintic PH curves are bounded and continuous as shown in Figure 7. Comparing Figure 10 with Figure 9, it can be found from Figure 10 that the angular jerks in the trajectory planning based on motion superposition have cusps, while the velocities, accelerations and jerks in joint space are bounded and continuous in Figure 9. Therefore, the trajectory planning based on quintic PH curves has more stable motion characteristics.

The cycle time T of the proposed two methods was also compared. When $0 \leq h \leq 0.3$m, $0 \leq w \leq 1$m, by subtracting the cycle time of the pick-and-place operation based on motion superposition from the cycle time of the pick-and-place operation based on quintic PH curves, the cycle time difference is demonstrated in Figure 11.

As can be seen from Figure 11, 99.70% of the cycle difference is negative. Therefore, the simulation results show that the trajectory planning method based on quintic PH curves has a shorter cycle time compared with the trajectory planning method based on motion superposition.

B. PROTOTYPE TEST
The experimental system includes host computer system of Delta robot, motion controller, servo system, mechanical structure, industrial camera and so on. The Delta robot's fixed platform radius is 150 mm, the moving platform radius is 51 mm, the active arm length is 325 mm and the slave arm length is 800 mm. Experiments were carried out on the prototype to test the performance and stability of the proposed two different trajectory planning methods. Figure 12 shows the experimental process. Figure 13 (a) and (b) show the actual angular velocities of the active joints, which are planned by the quintic PH curves and motion superposition trajectory planning methods, respectively. Figure 13 (c) and (d) show the torques in the motors, which are planned by the quintic PH curves and motion superposition trajectory planning
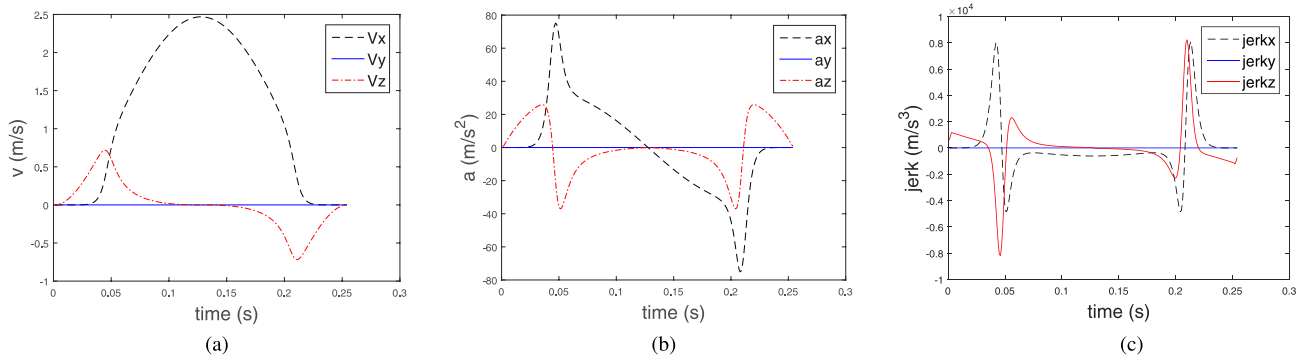
FIGURE 7. Velocities, accelerations and jerks of the end effector in Cartesian space with the trajectory planning based on quintic PH curves. (a) Velocities. (b) Accelerations. (c) Jerks.
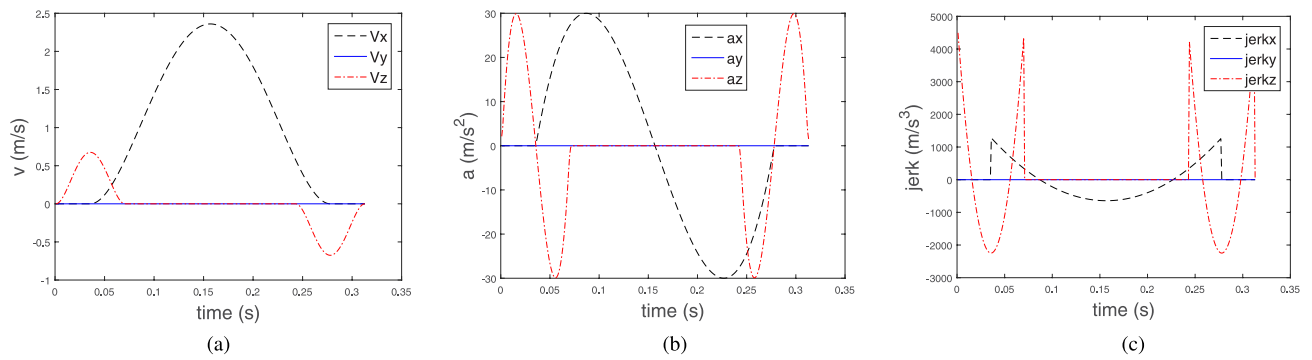

FIGURE 8. Velocities, accelerations and jerks of the end effector in Cartesian space with the trajectory planning based on motion superposition. (a) Velocities. (b) Accelerations. (c) Jerks.
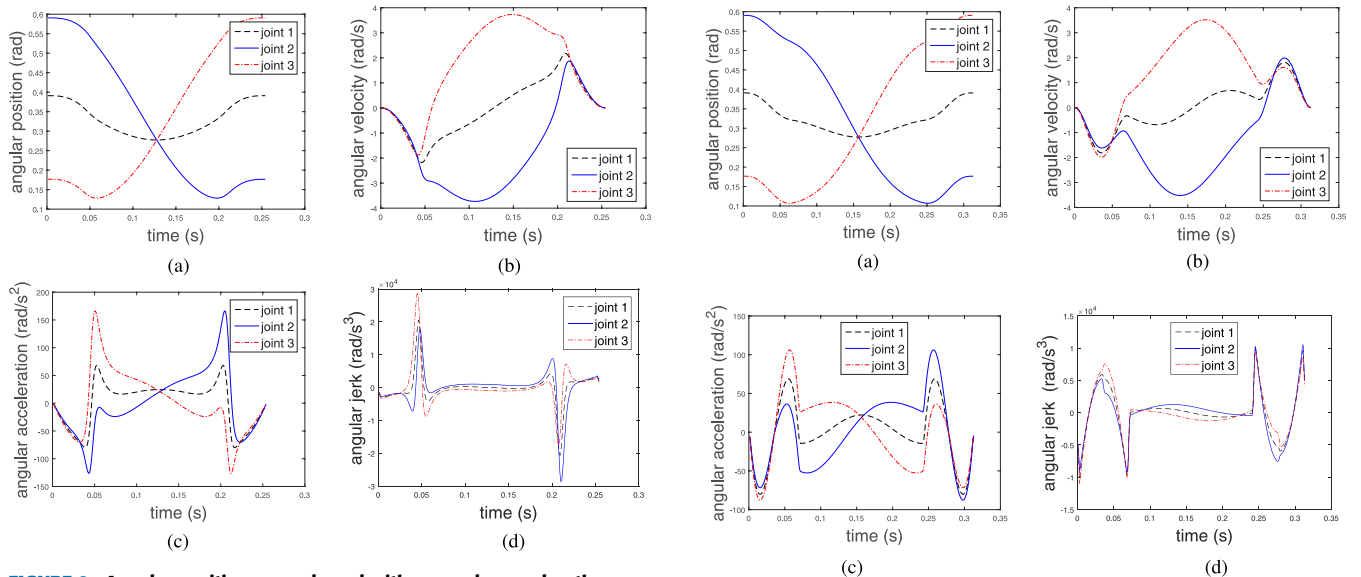

FIGURE 9. Angular positions, angular velocities, angular accelerations and angular jerks with the trajectory planning based on quintic PH curves. (a) Angular positions. (b) Angular velocities. (c) Angular accelerations. (d) Angular jerks.

FIGURE 10. Angular positions, angular velocities, angular accelerations and angular jerks with the trajectory planning based on motion superposition. (a) Angular positions. (b) Angular velocities. (c) Angular accelerations. (d) Angular jerks.

methods, respectively. The actual angular velocities were obtained by dividing the motor speed by the reduction ratio. The motor speed was measured by the speed monitor signal from the motor, and the motor torque was measured by the
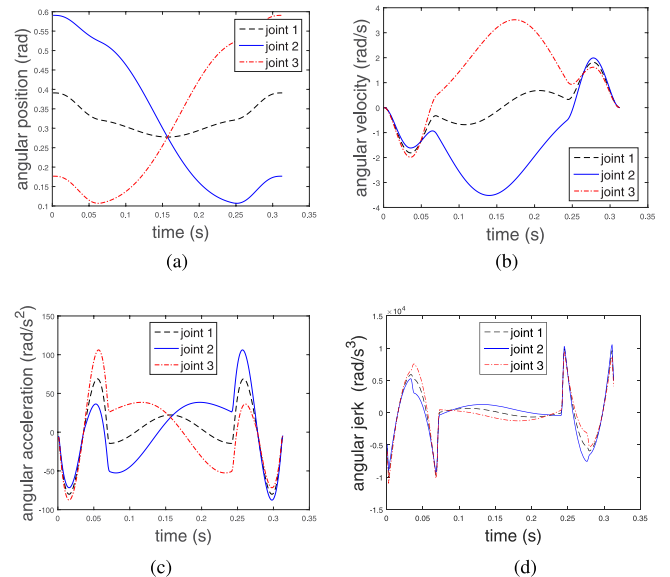
torque monitor signal from the motor. The angular velocities demonstrate that the proposed method has a shorter cycle

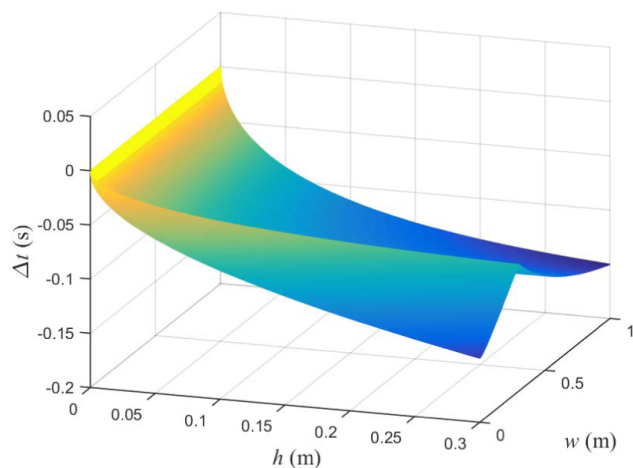**FIGURE 11.** Cycle time difference between the proposed two methods.

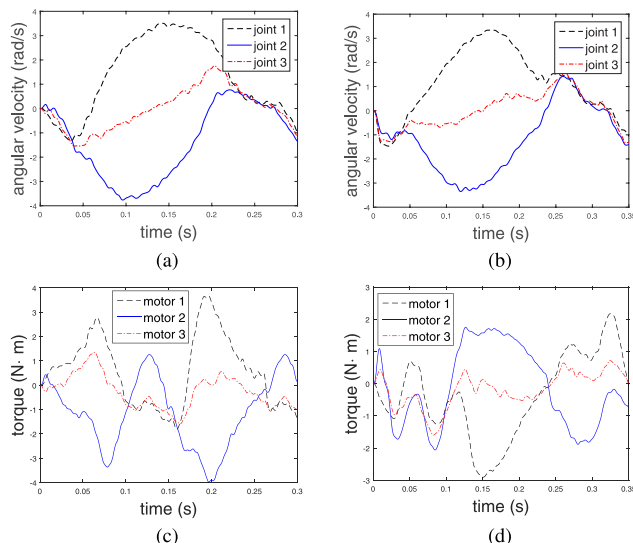**FIGURE 12.** Experimental process.

FIGURE 13. Actual angular velocities and torques of the proposed two methods. (a) Angular velocities with the trajectory planning based on quintic PH curves. (b) Angular velocities with the trajectory planning based on motion superposition. (c) Torques with the trajectory planning based on quintic PH curves. (d) Torques with the trajectory planning based on motion superposition.
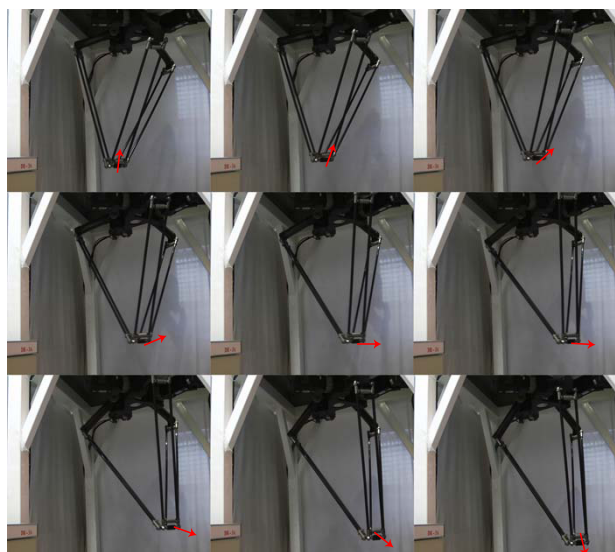
time than the comparison method. It can be observed from Figure 13 that torques in the comparison method change more frequently than torques in the proposed method. In addition, it can be deduced from the torques that the motors in the comparison method require a larger startup current than motors in the proposed method obviously.

It is found that the better results are obtained using the trajectory planning based on quintic PH curves by observing actual angular velocities, torques and cycle time. The trajectory planning based on quintic PH curves has the advantages of the shorter motion cycle time and more stable motion characteristics compared with the one based on motion superposition. Experimental results are consistent with the simulation results. Both the results of simulation and experiments reveal that the trajectory planning based on quintic PH curves contributes to high-speed operations of the Delta robot.

V. CONCLUSION

This study presents a time-optimal trajectory planning method based on quintic PH curves to gain a high-efficiency, smooth and stable performance for Delta parallel robot when performing high-speed operations. Conventionally, the trajectory planning based on vertical and horizontal motion superposition is mostly applied to trajectory planning of the pick-and-place operation for Delta robot. In order to reduce the motion cycle time and get a stable performance in the pick-and-place operation, the trajectory planning based on quintic PH curves is proposed by applying the quintic PH curves to the transition segments and optimizing the PH curves. The simulation results show that the trajectory planning based on quintic PH curves provides a shorter motion cycle and more stable motion performance compared with the trajectory planning based on motion superposition. Experiments were carried out on the prototype, which show that the proposed method is an efficient solution to the trajectory planning. Both the results of simulation and experiments reveal that the trajectory planning based on quintic PH curves contributes to high-speed pick-and-place operation of the Delta robot.

REFERENCES

[1] F. Pierrot, C. Reynaud, and A. Fournier, "DELTA: A simple and efficient parallel robot," *Robotica*, vol. 8, no. 2, pp. 105–109, 1990.
[2] L. Simionescu, L. Ciupitu, and L. C. Ionita, "Static balancing with elastic systems of *DELTA* parallel robots," *Mech. Mach. Theory*, vol. 87, pp. 150–162, May 2015.
[3] M. Furqan, M. Suhaib, and N. Ahmad, "Studies on stewart platform manipulator: A review," *J. Mech. Sci. Technol.*, vol. 31, no. 9, pp. 4459–4470, 2017.
[4] J. P. Merlet, *Parallel Robots*. New York, NY, USA: Springer-Verlag, 2012.
[5] B. Gherman, D. Pisla, C. Vaida, and N. Plitea, "Development of inverse dynamic model for a surgical hybrid parallel robot with equivalent lumped masses," *Robot. Comput. Integr. Manuf.*, vol. 28, no. 3, pp. 402–415, 2012.

[6] H. Cervantes-Culebro, C. A. Cruz-Villar, M.-G. M. Peñaloza, and E. Mezura-Montes, "Constraint-handling techniques for the concurrent design of a five-bar parallel robot," *IEEE Access*, vol. 5, pp. 23010–23021, 2017.

[7] J. Lin, C.-H. Luo, and K.-H. Lin, "Design and implementation of a new DELTA parallel robot in robotics competitions," *Int. J. Adv. Robot. Syst.*, vol. 12, no. 10, 2015, Art. no. 153.

[8] L. Feng, W. Zhang, Z. Gong, G. Lin, and D. Liang, "Developments of delta-like parallel manipulators—A review," *Robot*, vol. 36, no. 3, pp. 375–384, 2014.

[9] G. Borchert, M. Battistelli, G. Runge, and A. Raatz, "Analysis of the mass distribution of a functionally extended delta robot," *Robot. Comput. Integr. Manuf.*, vol. 31, pp. 111–120, Feb. 2015.

[10] M. Moghaddam and S. Y. Nof, "Parallelism of pick-and-place operations by multi-gripper robotic arms," *Robot. Comput. Integr. Manuf.*, vol. 42, pp. 135–146, Dec. 2016.

[11] K. Harada, T. Tsuji, K. Nagata, N. Yamanobe, and H. Onda, "Validating an object placement planner for robotic pick-and-place tasks," *Robot. Auto. Syst.*, vol. 62, no. 10, pp. 1463–1477, 2014.

[12] H. Abdellatif and B. Heimann, "Adapted time-optimal trajectory planning for parallel manipulators with full dynamic modelling," in *Proc. IEEE Int. Conf. Robot. Autom.*, Barcelona, Spain, Apr. 2005, pp. 411–416.

[13] L.-T. Schreiber and C. Gosselin, "Kinematically redundant planar parallel mechanisms: Kinematics, workspace and trajectory planning," *Mech. Mach. Theory*, vol. 119, pp. 91–105, Jan. 2018.

[14] S. Kucuk, "Optimal trajectory generation algorithm for serial and parallel manipulators," *Robot. Comput. Integr. Manuf.*, vol. 48, pp. 219–232, Dec. 2017.

[15] N. Zhang, W. Shang, and S. Cong, "Geometry-based trajectory planning of a 3-3 cable-suspended parallel robot," *IEEE Trans. Robot.*, vol. 33, no. 2, pp. 484–491, Apr. 2017.

[16] M. Afroun, T. Chettibi, and S. Hanchi, "Planning optimal motions for a DELTA parallel robot," in *Proc. IEEE Medit. Conf. Control Autom.*, Ancona, Italy, Jun. 2006, pp. 179–184.

[17] Z. Xie, D. Shang, and P. Ren, "Optimization and experimental verification of pick-and-place trajectory for a delta parallel robot based on Lamé curves," *J. Mech. Eng.*, vol. 51, no. 1, pp. 52–59, 2015.

[18] R. Choe, J. Puignavarro, V. Cichella, E. Xargay, and N. Hovakimyan, "Cooperative trajectory generation using pythagorean hodograph Bézier curves," *J. Guid. Control Dyn.*, vol. 39, no. 8, pp. 1744–1763, 2016.

[19] R. T. Farouki and T. Sakkalis, "Pythagorean hodographs," *IBM J. Res. Develop.*, vol. 34, no. 5, pp. 736–752, Sep. 1990.

[20] J. Shi, Q.-Z. Bi, L. Zhu, and Y. Wang, "Corner rounding of linear five-axis tool path by dual PH curves blending," *Int. J. Mach. Tools Manuf.*, vol. 88, pp. 223–236, Jan. 2015.

[21] A. A. Neto, D. G. Macharet, and M. F. M. Campos, "On the generation of trajectories for multiple UAVs in environments with obstacles," *J. Intell. Robot. Syst.*, vol. 57, nos. 1–4, pp. 123–141, 2010.

[22] B. Lotfi, Z. W. Zhong, and L. P. Khoo, "Prediction of cutting forces along pythagorean-hodograph curves," *Int. J. Adv. Manuf. Technol.*, vol. 43, nos. 9–10, pp. 872–882, 2009.

[23] K. M. Nittler and R. T. Farouki, "Efficient high-speed cornering motions based on continuously-variable feedrates. II. Implementation and performance analysis," *Int. J. Adv. Manuf. Technol.*, vol. 88, nos. 1–4, pp. 159–174, 2017.

[24] W. Zeng, J. Yi, X. Rao, and Y. Zheng, "A two-stage path planning approach for multiple car-like robots based on PH curves and a modified harmony search algorithm," *Eng. Optim.*, vol. 49, no. 11, pp. 1995–2012, 2017.

[25] R. T. Farouki and K. M. Nittler, "Efficient high-speed cornering motions based on continuously-variable feedrates. I. Real-time interpolator algorithms," *Int. J. Adv. Manuf. Technol.*, vol. 87, nos. 9–12, pp. 3557–3568, 2016.

[26] J. Jahanpour and B. M. Imani, "Real-time P-H curve CNC interpolators for high speed cornering," *Int. J. Adv. Manuf. Technol.*, vol. 39, nos. 3–4, pp. 302–316, 2008.

[27] G. Albrecht, C. V. Beccari, J.-C. Canonne, and L. Romani, "Planar pythagorean-hodograph B-spline curves," *Comput. Aided Geometric Des.*, vol. 57, pp. 57–77, Oct. 2017.

[28] J. Mei, J. Zang, Z. Qiao, S. Liu, and T. Song, "Trajectory planning of 3-DOF delta parallel manipulator," *J. Mech. Eng.*, vol. 52, no. 19, pp. 9–17, 2016.

[29] H. A. Rothbart, *CAM Design Handbook*. New York, NY, USA: McGraw-Hill, 2004.

[30] J. Angeles, *Fundamentals of Robotic Mechanical Systems*. New York, NY, USA: Springer, 2007.

[31] L. M. Zhang, "Integrated optimal design of delta robot using dynamic performance indeices," Ph.D. dissertation, Dept. Mech. Eng., Tianjin Univ., Tianjin, China, 2011.

[32] X. G. Lu, Y. Zhao, and M. Liu, "Self-learning interval type-2 fuzzy neural network controllers for trajectory control of a delta parallel robot," *Neurocomputing*, vol. 283, pp. 107–119, Mar. 2018.

[33] C.-T. Chen and T.-T. Liao, "A hybrid strategy for the time- and energy-efficient trajectory planning of parallel platform manipulators," *Robot. Comput. Integr. Manuf.*, vol. 27, no. 1, pp. 72–81, 2011.

[34] M. A. Laribi, L. Romdhane, and S. Zeghloul, "Analysis and dimensional synthesis of the DELTA robot for a prescribed workspace," *Mech. Mach. Theory*, vol. 42, no. 7, pp. 859–870, 2007.

[35] S. S. Ge, X. Liu, C.-H. Goh, and L. Xu, "Formation tracking control of multiagents in constrained space," *IEEE Trans. Control Syst. Technol.*, vol. 24, no. 3, pp. 992–1003, May 2016.

[36] J. Sun, J. Tang, and S. Lao, "Collision avoidance for cooperative UAVs with optimized artificial potential field algorithm," *IEEE Access*, vol. 5, pp. 18382–18390, 2017.

[37] Omron Corp. (2018). *Datasheet: Quattro 650H 650HS*. Accessed: May 11, 2018. [Online]. Available: https://industrial.omron.us/en/media/I265E-EN-01_Quattro_650H_650HS_Datasheet_tcm849-112091.pdf

TINGTING SU received the B.S. degree in automation from Central South University, Changsha, China, in 2013. She is currently pursuing the Ph.D. degree with the Institute of Automation, Chinese Academy of Sciences, Beijing, China. She is also with the University of Chinese Academy of Sciences, Beijing, China. Her research interests include trajectory planning, robotics and intelligent control systems.

LONG CHENG (SM'14) received the B.S. degree (Hons.) in control engineering from Nankai University, Tianjin, China, in 2004, and the Ph.D. degree (Hons.) in control theory and control engineering from the Institute of Automation, Chinese Academy of Sciences (IACAS), Beijing, China, in 2009.

In 2010, he was a Post-Doctoral Research Fellow with the Department of Mechanical Engineering, University of Saskatchewan, Saskatoon, SK, Canada, for eight months, and he was with the Mechanical and Industrial Engineering Department, Northeastern University, Boston, MA, USA, from 2010 to 2011. From 2013 to 2014, he was a Visiting Scholar with the Electrical and Computer Engineering Department, University of California at Riverside, Riverside, CA, USA. He is currently a Professor with the Laboratory of Complex Systems and Intelligent Science, IACAS. He has authored or co-authored over 50 technical papers in peer-refereed journals and prestigious conference proceedings. His research interests include intelligent control of smart materials, coordination of multiagent systems, neural networks, and their applications to robotics.

Dr. Cheng is an Editorial Board Member of *Neurocomputing* and the *International Journal of Systems Science*.

YUNKUAN WANG was born in 1966. He received the M.Sc. degree in industrial automation from the Harbin Institute of Technology, Harbin, China, in 1992. He is currently a Professor with the Institute of Automation, Chinese Academy of Sciences, Beijing, China. His research interests include intelligent robot, servo-vision control, and complex control systems.

JUN ZHENG was born in 1979. He received the Ph.D. degree in control theory and control engineering from the Institute of Automation, Chinese Academy of Sciences, Beijing, China, in 2009. He is currently an Associate Professor with the Institute of Automation, Chinese Academy of Sciences, Beijing, China. His research interests include intelligent robot and servo control and motion control systems.

XU LIANG received the B.S. degree in automation from Central South University, Changsha, China, in 2013. He is currently pursuing the Ph.D. degree with the Institute of Automation, Chinese Academy of Sciences, Beijing, China. He is also with the University of Chinese Academy of Sciences, Beijing, China. His research interests include rehabilitation robot, human machine interface, and interaction control.

HAOJIAN ZHANG received the M.Sc. degree in control theory and control engineering from the Qingdao University of Science and Technology, Qingdao, China, in 2013. He is currently pursuing the Ph.D. degree with the Institute of Automation, Chinese Academy of Sciences, Beijing, China. His research interests include optimization algorithms, robotics, and path planning.

● ● ●